RESEARCH ARTICLE | MARCH 14 2024

# Opto-electrochemical variation with gel polymer electrolytes in transparent electrochemical capacitors for ionotronics

Chandini Kumar ; Arun K. Sebastian ; Prasutha Rani Markapudi ; Mustehsan Beg ;
Senthilarasu Sundaram ; Amir Hussain ; Libu Manjakkal ✉

Check for updates

CrossMark

View Online

Export Citation

21 March 2024 14:35:48

# Opto-electrochemical variation with gel polymer electrolytes in transparent electrochemical capacitors for ionotronics ⓕ sci
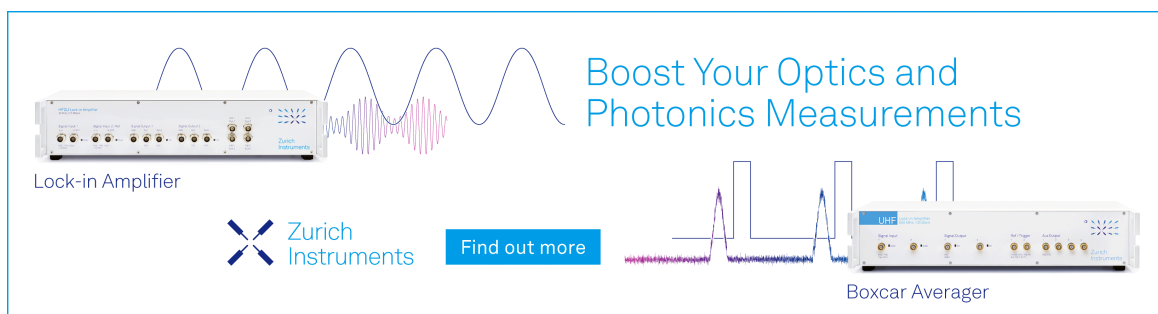
Chandini Kumar, ⓘ Arun K. Sebastian, ⓘ Prasutha Rani Markapudi, ⓘ Mustehsan Beg, ⓘ Senthilarasu Sundaram, ⓘ Amir Hussain, ⓘ and Libu Manjakkal[a) ⓘ

**AFFILIATIONS**

School of Computing and Engineering and the Built Environment, Edinburgh Napier University, Merchiston Campus, EH10 5DT Edinburgh, United Kingdom

[a)]Author to whom correspondence should be addressed: L.Manjakkal@napier.ac.uk

**ABSTRACT**

Advanced flexible ionotronic devices have found excellent applications in the next generation of electronic skin (e-skin) development for smart wearables, robotics, and prosthesis. In this work, we developed transparent ionotronic-based flexible electrochemical capacitors using gel electrolytes and indium tin oxide (ITO) based transparent flexible electrodes. Different gel electrolytes were prepared using various salts, including NaCl, KCl, and LiCl in a 1:1 ratio with a polyvinyl alcohol (PVA) solution and compared its electrochemical performances. The interaction between gel electrolytes and ITO electrodes was investigated through the development of transparent electrochemical capacitors (TEC). The stable and consistent supply of ions was provided by the gel, which is essential for the charge storage and discharge within the TEC. The total charge contribution of the developed TECs is found from the diffusion-controlled mechanism and is measured to be 4.59 mC cm$^{-2}$ for a LiCl/PVA-based gel. The prepared TEC with LiCl/PVA gel electrolyte exhibited a specific capacitance of 6.61 mF cm$^{-2}$ at 10 $\mu$A cm$^{-2}$. The prepared electrolyte shows a transparency of 99% at 550 nm and the fabricated TEC using LiCl/PVA gel exhibited a direct bandgap of 5.34 eV. The primary benefits of such ionotronic-based TEC development point to its potential future applications in the manufacturing of transparent batteries, electrochromic energy storage devices, ionotronic-based sensors, and photoelectrochemical energy storage devices.

Transparent, smart, and intelligent flexible ionotronic devices have gained significant attention in many fields including wearables[1] and robotics.[2] These applications required flexible ionotronic components, including ionic skins,[3] electroluminescence,[4] transparent actuators, such as loudspeakers,[5] and touchpads and displays,[6,7] in which transparency and electrochemical performances play a key role. Electrochemical capacitors act as a crucial component for these transparent devices whose function is based on an ionotronics mechanism where both mobile ions and electrons are involved in reactions. Such electrochemical capacitors could act as mechanoreceptors such as capacitive sensors for touch, and temperature monitoring, and will also function as an energy source.[8] For the development of such transparent electronic components including sensors and energy storage devices, the variation of optical and electrochemical properties of transparent electrodes with a gel polymer electrolyte is highly important for its sensing, visual effect, and energy-storing capability. There

are three major mechanisms, including electric double layer (EDL), electrochemical reaction, and ionic diffusions involved in ionotronic components.[9,10] In this context, the interaction of the ionic gel with conductive or active electrodes is of utmost importance for establishing the actual mechanism.

The selection of electrolytes presents a critical challenge in the development of transparent electrochemical devices, as it requires a delicate balance to simultaneously achieve optimal ion-storing, efficiency, and transparency.[11] The electrolyte must remain stable over extended periods to ensure long-term reliable performance of the devices. However, some transparent electrolyte materials may be more susceptible to degradation or have limited stability, posing challenges over time when attempting to maintain optimal electrochemical performance.[12] Polymer-based gel electrolytes are essential in the fabrication of ionotronic devices that have a high water content and can retain a significant amount of electrolyte solution.[13,14] For various types of

ionotronic devices, different types of polymer gel electrolytes are implemented which include polyacrylamide (PAAM), polyvinyl alcohol (PVA)/tannic acid functionalized nanocellulose (PVA/TA@s-NC) hydrogels and poly-(acrylamide-co-acrylic acid) p(AM-co-AA) hydrogel mixed with zinc ion ($Zn^{2+}$) and aluminum ion ($Al^{3+}$).[15] The exceptional physical, mechanical, and chemical properties of the polymers play a pivotal role in influencing ionic conductivity, as the dissolved ions within the polymer gel predominantly determine its contribution to the development of an electrochemical device. In addition to electrolytes, the interaction of electrolytes with the electrode surface plays a crucial role in the formation of electrochemical processes. The type of electrode, including metal oxides, graphene, conducting polymers, or composites significantly influences the electrode's performance.[16]

In this work, we developed transparent electrochemical capacitors (TEC) as an ionotronic device, and their optical and electrochemical properties were investigated. Here, we developed TECs based on indium tin oxide (ITO) coated on the top of polyethylene terephthalate (PET) substrate with NaCl/PVA, KCl/PVA, and LiCl/PVA gel polymer electrolytes, as illustrated in Fig. 1(a) and the fabricated device in Fig. 1(b). Here, ITO/PET which functions as a current collector/substrate exhibits more than 90% of transparency and extremely low sheet resistance (0.0001 $\Omega\,cm^{-1}$) due to the high bandgap and free career density.[17] The interaction of electrolyte ions with these ITO electrodes is the key factor in designing the performance of the ionotronic devices. ITO is used to fabricate flexible electrochemical devices and to further enhance the performances of multiple materials that were coated in previous works.[18] In this present work, different polymer gel electrolytes are prepared by use of NaCl, KCl, and LiCl in a 1:1 ratio with a PVA solution. Polymer gel ensures a stable and consistent supply of ions, which are essential for the charge storage and discharge processes within the TEC. The polymer gel layer can serve as an ionic conductive channel and as a separator between the two electrodes in TECs.

Additionally, polymer gels can retain moisture and prevent evaporation of the electrolyte solution.[7,14,19] This property ensures the long-term stability and consistent performance of the TECs. The experimental details of the device fabrication and characterization are given in the supplementary material. The electrochemical properties of the TEC could be varied while applying an external force on the top of this TEC, as shown in Fig. 1(c) due to variations in gel electrolyte distribution.

A microcrystalline with nano-porous has great advantages in electrode–gel interaction in TEC development. Figure 1(d) illustrates the SEM image of the ITO film revealing uniform coated microstructure films with nano-porous and regularly distributed grains. Contact angle measurements [Fig. 1(e)] are conducted to evaluate the wettability of the ITO film with a mean contact angle of 72.44°. These findings suggest that the ITO film exhibits enhanced wettability, indicating a hydrophilic character with a pronounced attraction to water and polar electrolytes. This attribute facilitates efficient liquid absorption and concurrently reduces the internal resistance of energy storage devices.

The transparency of the polymer gel electrolyte is measured through the optical transmittance spectra for NaCl/PVA, KCl/PVA, and LiCl/PVA in the 300–800 nm range and is shown in Fig. 1(f). A distinct absorption is evident below the 400 nm region, accompanied by a rapid reduction as the wavelengths decrease toward the visible region in all three electrolytes. Following this, LiCl/PVA and KCl/PVA exhibited transmittance values of approximately 98.32% and 98.08%, respectively. At the same wavelength (400 nm), NaCl/PVA demonstrated a transmittance of around 95.26%. Within the wavelength range of 550 nm, all other polymer gel electrolytes (KCl and LiCl) displayed ~100% transmittance, except for NaCl/PVA which achieved a transmittance of 99%. Subsequently, the transmission levels stayed relatively low. The vibrational modes of molecules in a sample, which provide information about the chemical composition and interactions within the sample, are analyzed using Fourier transform infrared



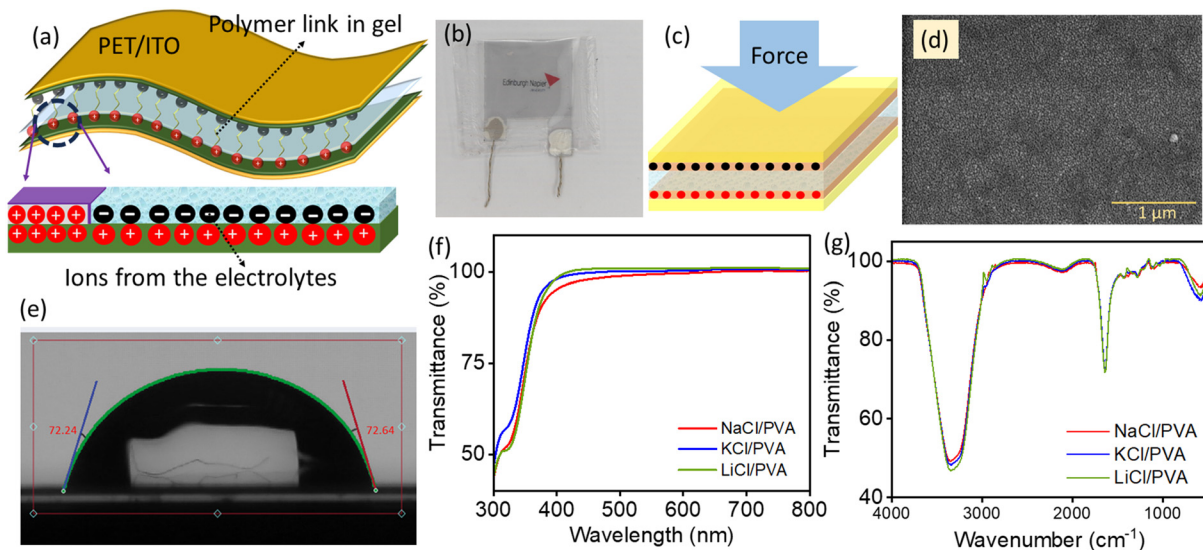**FIG. 1.** (a) Schematic representation of the TEC for transparent ionotronic devices with the ionic distribution shown in the magnified image. (b) Image of the developed TEC. (c) Schematic representation of TEC under external force. (d) SEM image of the ITO film, (e) contact angle measurement of the ITO with electrolyte, (f) UV-transmittance spectra of the polymer gel electrolyte (g), and FTIR spectra of the polymer gel electrolyte.

spectroscopy (FTIR). The results of FTIR analysis on different polymer gel electrolytes composed of PVA and various salts (NaCl, KCl, LiCl). The FTIR spectra [Fig. 1(g)] for these compositions show certain characteristic absorption peaks, which reveal important information about the interactions occurring within the gel electrolyte. At $3330\,cm^{-1}$, an absorption peak is observed in all the gel electrolytes and corresponds to the –OH stretching vibrational band of alcohols. This observation indicates hydrogen-bond associations within the PVA molecules in the gel. Hydrogen bonding is a common interaction in polymer systems, and its presence suggests that the PVA chains are similarly interacting with each other in all the gel compositions. A small peak at $2880\,cm^{-1}$ is specifically observed in the FTIR spectra of gel electrolytes containing LiCl. It arises from the stretching vibrations of the –$CH_3$ groups, which are likely present in these specific salts or result from their interaction with the PVA matrix. The peak is seen at $1638\,cm^{-1}$ in the FTIR spectra of all gel electrolytes, indicating the presence of a carboxyl group within the system. This group is likely part of the PVA or may arise from the interaction of PVA with different salts used in the compositions.

The ionic conductivity of polymer gel electrolytes plays a pivotal role in determining the electrochemical properties of ionotronic devices. Here, polymer gel electrolytes characterized by heightened ionic conductivity possess an expanded electrochemical window, consequently enhancing TEC efficiency. It is worth noting that polymer gel electrolytes with elevated ionic conductivity demonstrate commendable performance even in low-temperature environments. Figure 2(a) shows a comparative view of the ionic conductivity across NaCl, KCl, and LiCl-based polymer gel electrolytes. The analysis revealed that

PVA/KCl gel demonstrates exceptional ionic conductivity, measuring approximately $98.8\,mS\,cm^{-1}$. Electrochemical impedance spectroscopy (EIS) analysis was carried out to analyze electrode–electrolyte interaction in TEC. In Figs. 2(b)–2(d), the Nyquist plot illustrates the response of the ITO electrode to NaCl, KCl, and LiCl based gel electrolytes. In the EIS profile of the LiCl polymer gel electrolyte, an evident pattern emerges as a semicircle indicating a reduced capacitance is noticeable in the high-frequency domain, complemented by a linear trend at lower frequencies, as can be observed in this plot. These semicircular patterns signify the presence of an interfacial charge transfer resistance between the electrode and electrolyte systems, regardless of the specific electrolyte employed. This charge transfer resistance could be due to the ITO electrode resistance and its contact resistance to the gel electrolyte. This represents pseudocapacitance of the material due to the faradaic reactions.[20]

Furthermore, the EIS profiles illustrated in Figs. 2(b)–2(d) exhibit substantial deviations from the imaginary axis across all electrolytes. This divergence is indicative of ionic diffusion into the electrode's pores, reinforcing the suggestion of the electrode's capacitive nature within these electrolytes. The high-frequency region within the spectra provides valuable information about the solution resistance ($R_s$). The $R_s$ values observed for NaCl, KCl, and LiCl-based polymer gel were 12.17, 25.8, and $15.72\,\Omega\,cm^{-2}$, respectively. PVA/NaCl with ITO exhibits greater conductivity than PVA/KCl and PVA/LiCl with ITO due to its lower solution resistance. The magnitude of impedance variation with frequency for TECs with various gel electrolytes is represented through the Bode impedance plot as shown in Fig. 2(e). It was observed that when subjected to such high frequencies, the device
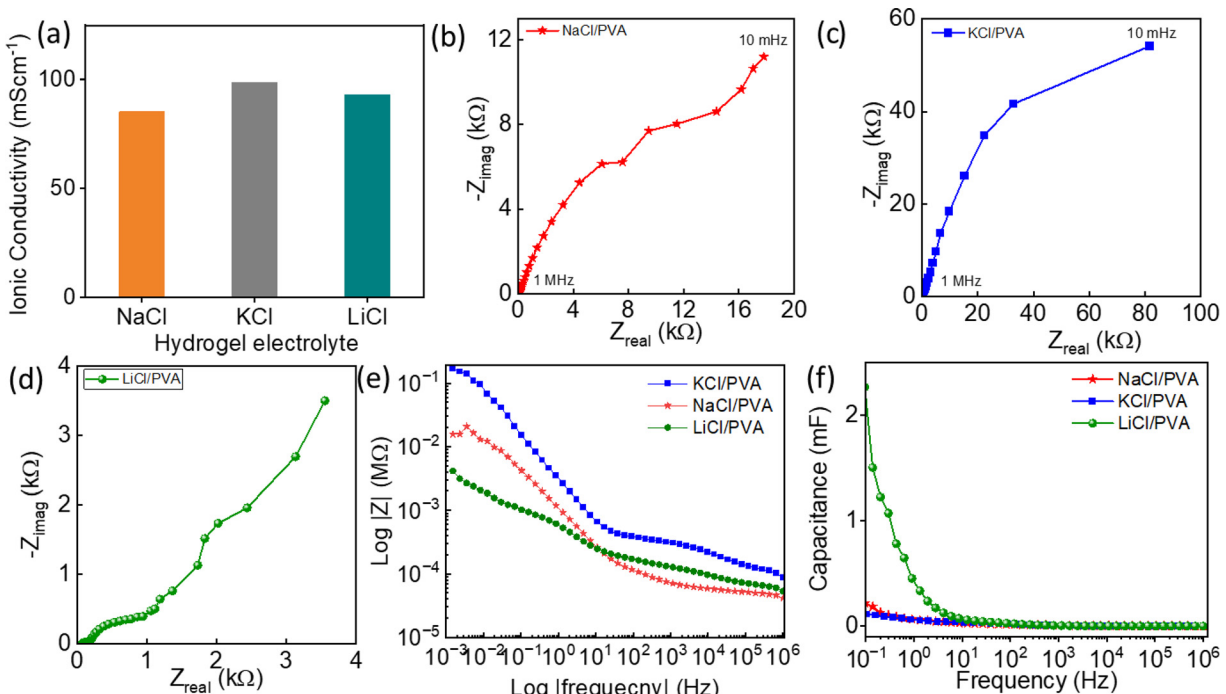


**FIG. 2.** (a) Ionic conductivity of electrolytes and (b)–(d) Nyquist plot for the TECs based on NaCl, KCl, and LiCl, respectively. (e) Bode impedance plot for the TECs with various gel electrolytes and (f) capacitance variation found through EIS analysis for TECs.

exhibits a behavior like that of a basic resistor. However, in low-frequency regions, the diffusion of electrolyte ions ($Li^+$, $K^+$, or $Na^+$) into the active ITO electrode leads to impedance characteristics.[21] The PVA/LiCl-based TEC shows a lower resistance value in a lower frequency range and it confirms the Bode impedance plot in Fig. 2(e). These ionic movements and the lower resistance of the electrodes reveal its high capacitance in the low-frequency range, which is given in Fig. 2(f). The capacitance value demonstrates that in the lower frequency region, the device exhibited a maximum value of capacitance and decreased with an increasing frequency, and in the high frequency range, it shows a constant value that reveals the porous nature of the film.

The ionic interaction of the electrode with the electrolyte was investigated using cyclic voltammetry (CV) analysis. CV analysis predicts the stability of the complexed transition metal oxidation state, reversibility of electron transfer processes, total charge storage, and its contribution and reactivity of the polymer gel electrolytes with ITO electrodes. The CV analysis shows that depending on the type of electrolyte, the electrode–electrolyte interaction varies, and it leads to the formation of pseudocapacitive behavior of the CV curve. Figure 3(a) shows the CV curves for TEC developed using LiCl-based polymer gel electrolytes in a scan rate of $5\text{--}1000\,\text{mV s}^{-1}$. The CV curve for NaCl and KCl based TECs given in Figs. S1(a) and S1(b) in the supplementary material. The CV curve shows a quasi-rectangular shape, and such shape is normal in pseudocapacitance due to the redox reaction of the material.[22,23] The specific capacitance of the TECs are measured from the CV analysis using the expression reported in previous works.[22] The measured value of specific capacitance for the TECs is

given in Fig. 3(b). The measurement shows LiCl/PVA gel-based TEC exhibit high specific capacitance $2.17\,\text{mF cm}^{-2}$ at $5\,\text{mV s}^{-1}$ and the capacitance decrease exponentially with increasing scan rate. This observation highlights the LiCl gel electrolyte as a promising candidate for enhancing the charge storage capabilities of ITO-coated electrodes in electrochemical applications. Notably, the TEC integrated with the LiCl polymer gel electrolyte achieved $254.21\,\mu\text{F cm}^{-2}$ specific capacitance is three times higher than for KCl-based polymer gel electrolytes and is $87.37\,\mu\text{F cm}^{-2}$ at $100\,\text{mV s}^{-1}$. The high capacitance value of LiCl-based TEC in the range of $\mu\text{F cm}^{-2}$ at high scan rates ($1\,\text{V s}^{-1}$) [from Fig. 3(b)] and in high frequency ($1\,\text{kHz}$) [Fig. 2(f)] shows that it is 1000 times higher than that of parallel-plate capacitive sensors (which is in the range of $\text{pF cm}^{-2}$), indicating the high sensitivity implication of TEC for a electromechanical sensors.[9] The high capacitance value is due to the charge storage properties of the polymer gel electrolyte–electrode interaction. Furthermore, the CV analysis was also used for measuring the charge contribution. The plot in Fig. 3(c) for logarithmic scan vs logarithmic current for a TEC in LiCl shows a slope of 0.44 for a low scan rate ($5\text{--}100\,\text{mV s}^{-1}$) ($R^2 = 0.999$), and it predicts that charge storage contribution is mainly due to the diffusion-controlled reaction. It was reported that for slope of 1, the device will exhibit capacitive contribution, for slope of 0.5 or below the device will be diffusion-controlled mechanism and slope between 1 and 0.5 is combined diffusion-controlled contribution and capacitive contribution.[24] Hence, the total charge contribution ($Q_t$) will be here from diffusion-controlled mechanism and is measured for LiCl/PVA as shown in Fig. 3(d) using expression S3 given in the supplementary material.
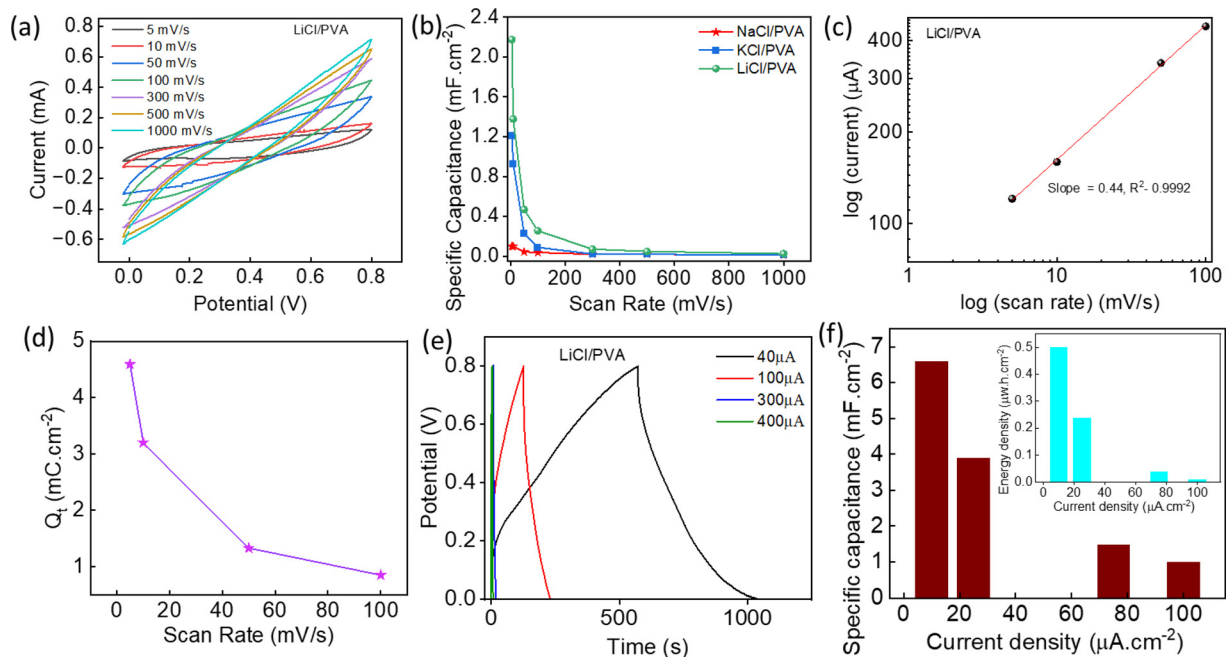


**FIG. 3.** (a) CV curves for LiCl-based TEC in different scan rates. (b) Specific capacitance variation with a scan rate of TECs in different electrolytes. (c) Plot for log(current) vs log scant rate for LiCl/PVA-based TEC to find the charging storing mechanism. (d) The total charge contribution of the TEC-based LiCl/PVA in different scan rates (e). The GCD curves for LiCl-based TEC (f) show the specific capacitance variation of LiCl/PVA-based TECs and the inset shows the energy density variation of the same device at different current densities.

The energy-storing ability of such TEC was investigated through the galvanostatic charge–discharge (GCD) analysis of the fabricated TECs and is given in Fig. 3(e) (for LiCl), Figs. S2(a) (NaCl) and S2(b) (for KCl). The GCD curves for the TEC with NaCl electrolyte were observed without any potential drift. However, the charge storing ability of this device is low and it discharges quickly. The rapid charge and discharge process is made possible by the electro-chemisorption of $Na^+$ cations at the negative electrode and $Cl^-$ anions at the positive electrode. During the analysis of the GCD behavior of KCl in the gel electrolyte, a consistent pattern was observed across all current densities. Notably, at a current density of 80 $\mu A$, a higher voltage drop was observed in Fig. S2(b). Conversely, as the current density was reduced, the charging time of the device increased, and it was evident that the voltage drop decreased accordingly. In Fig. 3(f), the charge–discharge performance of a TEC utilizing PVA/LiCl electrolyte is depicted. At lower current densities, the device exhibited minimal voltage drop during the discharge process. The inclusion of LiCl in the electrolyte facilitated linear charging and discharging behavior, indicating a stable and predictable operation for the device. Table S1 in the supplementary material presents the results obtained by calculating the specific capacitance, energy density, and power density using GCD measurements for the TECs. Upon a thorough analysis of the data presented in Table S1, a noticeable trend emerges: the specific capacitance and energy density both display a decline in response to the magnitude of the applied current. At lower current density, the TECs obtained maximum capacitance and energy density. In contrast to this behavior, the power density showcases a distinct and recognizable pattern of reversibility. This suggests that the power output of the TECs exhibits a consistent and reversible variation in relation to the changing current conditions, a phenomenon that underscores the dynamic nature of the power delivery capability of this gel based TECs. In comparison to gel electrolytes containing NaCl and KCl, the usage of LiCl gel electrolytes in TECs revealed superior performance. The specific capacitance measurements obtained under a constant current density of 10 $\mu A\,cm^{-2}$ reveal the performances 46.11 $\mu F\,cm^{-2}$ for NaCl/PVA, 1.61 mF $cm^{-2}$ for KCl/PVA, and 6.61 mF $cm^{-2}$ for LiCl/PVA based TECs, and it clearly shows this noticeable difference in performance. The application of LiCl-based gel as electrolytes significantly enhanced the overall performance of the TECs utilizing ITO electrodes. This enhancement resulted in a substantially higher specific capacitance value, reaching approximately 6.605 mF $cm^{-2}$ at 40 $\mu A$ (10 $\mu A\,cm^{-2}$). The variation of the specific capacitance and energy density with current density for the TEC based on LiCl/PVA is shown in Fig. 3(f). We also measured the energy and power density for the TECs at 10 $\mu A\,cm^{-2}$. TEC with NaCl/PVA exhibited 3.08 nWh $cm^{-2}$ and 3.47 $\mu W\,cm^{-2}$ of energy and power density. For instance, the TEC with NaCl/PVA exhibited .08 $\mu Wh\,cm^{-2}$ and 3.01 $\mu W\,cm^{-2}$ of energy and power density. By comparing the two TECs, we noticed that TEC-based LiCl/PVA exhibited high energy and power densities of 0.504 $\mu Wh\,cm^{-2}$ and 3.71 $\mu W\,cm^{-2}$, respectively. This result demonstrates the significant potential of LiCl gel as an efficient electrolyte for enhancing the energy storage capacities of these electrochemical capacitor systems. The repeatability in performance is checked for the TEC with a LiCl/PVA electrolyte-based device and carried out using CV, which is given in Fig. S3. It was noticed that there are significant challenges in the repeatability performance of devices, which strongly depend on the amount of electrolyte and the packaging method.

In the analysis of energy storage systems to assess their efficiency and overall performance, one crucial and fundamental factor that requires examination is the bandgap energy of gel electrolytes. This parameter plays a pivotal role in understanding how effectively the energy storage system can operate, as it impacts the behavior of the electrolyte material, influencing its conductivity and charge transport properties. The findings regarding the energy bandgap associated with direct electronic transitions (x = 2) are presented graphically in Fig. 4(a). This figure illustrates the relationship between $(\alpha h\nu)^2$ and photon energy ($h\nu$) to extract the direct bandgap values. In the context of this current research study, we have ascertained the direct bandgap values for different gel electrolytes. For the LiCl-based gel electrolyte, our analysis has yielded a bandgap value of 5.37 eV. Subsequently, we found that the KCl-based gel electrolyte possesses a direct bandgap of 5.35 eV, and the NaCl-based gel electrolyte exhibits a direct bandgap of 5.34 eV. It was found that the TEC with further modification using conjugated polymers or other metal oxides, will be an excellent candidate for electrochromic energy storage devices.[25,26] For such an energy storage device the bandgap could control the electrochromic and optical properties. The influence of polymeric material and n-type or p-type semiconductors influences the variation of the bandgap.[25,27] Here, we used a similar active electrode and PVA polymer and noticed that salts within the gel in this work are not strongly influencing the variation of the bandgap.

Finally, we tested the variation of electrochemical properties through the CV analysis (100 mV $s^{-1}$) under an external force on the top of the TEC, which was fabricated using LiCl/PVA as shown in Fig. 4(b). We applied static force to the top of the TEC, and it was noticed that with increasing the applied force, the peak current of the device enhanced. This variation in peak current in the CV curve could be due to the changing gel electrolyte distribution under the device due to the external force, which varies the ionic distribution. The capacitance of this TEC was measured using the area under the CV curve, and it was noticed that as the applied force increased, the capacitance of the TEC increased. The relative change in capacitance of the TEC under different applied forces is given in Fig. 4(c). This will lead to implementing the TEC with a gel electrolyte for ionotronic based pressure monitoring sensors, and further studies are required on this aspect. The leakage of the gel with external force will influence the performance, and to overcome this, appropriate packaging and TEC with a solid electrolyte is necessary.

In summary, here we focused on the electrochemical and optical characteristics of diverse gel electrolytes applied to ITO films. Three distinct polymer gel electrolytes, involving PVA in conjunction with NaCl, KCl, and LiCl, were meticulously prepared at a 1:1 ratio. By employing these electrolytes, symmetrical TECs were fabricated, using ITO films measuring 4 $cm^2$ in the surface area. Among these configurations, the PVA/LiCl-based TEC exhibited superior electrochemical performance and optical transparency when compared to the other electrolytes (NaCl and KCl). This specific configuration showcased a remarkable specific area capacitance of 6.61 mF $cm^{-2}$ at 10 $\mu A\,cm^{-2}$, underscoring the remarkable potential of LiCl gel as an efficient electrolyte capable of amplifying the energy storage capabilities of electrochemical capacitor systems. However, it is essential to acknowledge the limitations and challenges that surfaced during this exploration. Despite the electrolyte's gel-based nature, issues such as leakage during device fabrication were encountered. Addressing these challenges is imperative to develop a promising TEC design. The high capacitance value of LiCl gel-based TEC in the range of $\mu F\,cm^{-2}$ in high scan rate
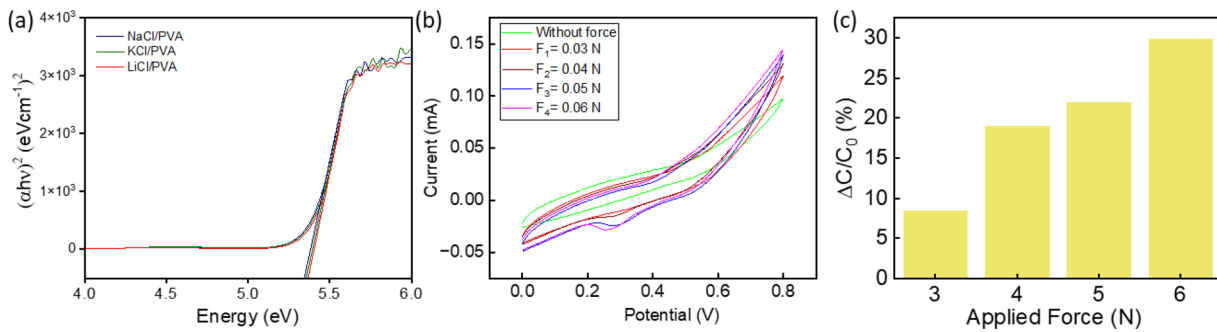
**FIG. 4.** (a) Bandgap energy measurement for TEC based on different polymer gels. (b) CV curve of TEC under various forces. (c) The relative change in capacitance of the TEC with applied force.

$(1\,\mathrm{V\,s^{-1}})$ and in high frequency (1 kHz) predicts its excellent performances for ionotronic based sensors and energy storage devices. The major advantages of such ionotronic based TEC development is its implementation in the fabrication of future transparent energy storage devices such as batteries, electrochromic energy storage and photoelectrochemical energy storage device and also various types of sensors.

See the supplementary material for the experimental details and figures related to results and discussion of NaCl and KCl based TECs.

## AUTHOR DECLARATIONS
### Conflict of Interest

The authors have no conflicts to disclose.

### Author Contributions

**Chandini Kumar:** Data curation (equal); Formal analysis (lead); Investigation (equal); Methodology (equal); Writing – original draft (lead). **Arun K. Sebastian:** Formal analysis (equal); Investigation (equal); Methodology (equal). **Prasutha Rani Markapudi:** Formal analysis (equal); Investigation (equal). **Mustehsan Beg:** Formal analysis (equal); Investigation (equal); Methodology (equal); Writing – review & editing (equal). **Senthilarasu Sundaram:** Investigation (equal); Writing – review & editing (equal). **Amir Hussain:** Investigation (equal); Writing – review & editing (equal). **Libu Manjakkal:** Conceptualization (lead); Data curation (equal); Formal analysis (equal); Funding acquisition (lead); Investigation (equal); Methodology (equal); Project administration (lead); Supervision (lead); Writing – original draft (equal); Writing – review & editing (lead).

## DATA AVAILABILITY

The data that support the findings of this study are available from the corresponding author upon reasonable request.

## REFERENCES

[1]S. Lee, S. Franklin, F. A. Hassani, T. Yokota, M. O. G. Nayeem, Y. Wang, R. Leib, G. Cheng, D. W. Franklin, and T. Someya, Science **370**(6519), 966 (2020);

J. H. Kim, K. G. Cho, D. H. Cho, K. Hong, and K. H. Lee, Adv. Funct. Mater. **31**(16), 2010199 (2021).
[2]C. Larson, B. Peele, S. Li, S. Robinson, M. Totaro, L. Beccai, B. Mazzolai, and R. Shepherd, Science **351**(6277), 1071 (2016); Z. Shen, X. Zhu, C. Majidi, and G. Gu, Adv. Mater. **33**(38), 2102069 (2021); L. E. Osborn, A. Dragomir, J. L. Betthauser, C. L. Hunt, H. H. Nguyen, R. R. Kaliki, and N. V. Thakor, Sci. Rob. **3**(19), eaat3818 (2018).
[3]M. Zhang, R. Yu, X. Tao, Y. He, X. Li, F. Tian, X. Chen, and W. Huang, Adv. Funct. Mater. **33**(10), 2208083 (2023).
[4]C. Dai, Y. Wang, Y. Shan, C. Ye, Z. Lv, S. Yang, L. Cao, J. Ren, H. Yu, and S. Liu, Mater. Horiz. **10**(1), 136 (2023); C. H. Yang, B. Chen, J. Zhou, Y. M. Chen, and Z. Suo, Adv. Mater. **28**(22), 4480 (2016); X. Ming, J. Du, C. Zhang, M. Zhou, G. Cheng, H. Zhu, Q. Zhang, and S. Zhu, ACS Appl. Mater. Interfaces **13**(34), 41140 (2021); S. H. Hong, Y. M. Kim, and H. C. Moon, ACS Appl. Mater. Interfaces **15**, 28516 (2023).
[5]C. Yang and Z. Suo, Nat. Rev. Mater. **3**(6), 125 (2018); K. Jia, X. Li, and Y. Wang, Soft Matter **17**(4), 834 (2021); J. Vaicekauskaite, C. Yang, A. L. Skov, and Z. Suo, Extreme Mech. Lett. **34**, 100597 (2020); W. Niu and X. Liu, Macromol. Rapid Commun. **43**(23), 2200512 (2022).
[6]R. Huo, G. Bao, Z. He, X. Li, Z. Ma, Z. Yang, R. Moakhar, S. Jiang, C. Chung-Tze-Cheong, and A. Nottegar, Adv. Funct. Mater. **33**, 2213677 (2023).
[7]W. Wang, Y. Liu, S. Wang, X. Fu, T. Zhao, X. Chen, and Z. Shao, ACS Appl. Mater. Interfaces **12**(22), 25353 (2020).
[8]Y. Wang, K. Jia, S. Zhang, H. J. Kim, Y. Bai, R. C. Hayward, and Z. Suo, Proc. Natl. Acad. Sci. **119**(4), e2117962119 (2022); E. M. Stewart, S. Narayan, and L. Anand, J. Mech. Phys. Solids **173**, 105196 (2023); X. Zhang, C. Cui, S. Chen, L. Meng, H. Zhao, F. Xu, and J. Yang, Chem. Mater. **34**(3), 1065 (2022).
[9]C. Wan, K. Xiao, A. Angelin, M. Antonietti, and X. Chen, Adv. Intell. Syst. **1**(7), 1900073 (2019).
[10]B. Yao, S. Wu, R. Wang, Y. Yan, A. Cardenas, D. Wu, Y. Alsaid, W. Wu, X. Zhu, and X. He, Adv. Funct. Mater. **32**(10), 2109506 (2022); K. Xiao, C. Wan, L. Jiang, X. Chen, and M. Antonietti, Adv. Mater. **32**(31), 2000218 (2020).
[11]X. Guan, L. Pan, and Z. Fan, Membranes **11**(10), 788 (2021).
[12]L. Zhao, Y. Li, M. Yu, Y. Peng, and F. Ran, Adv. Sci. **10**(17), 2300283 (2023).
[13]C. Y. Chan, Z. Wang, H. Jia, P. F. Ng, L. Chow, and B. Fei, J. Mater. Chem. A **9**(4), 2043 (2021).
[14]B. Ying and X. Liu, Iscience **24**(11), 103174 (2021).
[15]J. Du, C. Yue, Z. Zhang, Z. Liao, H. Tan, N. Li, J. Xu, Z. Tang, and L. Xu, Mater. Today Chem. **33**, 101658 (2023).
[16]V. C. Lokhande, A. C. Lokhande, C. D. Lokhande, J. H. Kim, and T. Ji, J. Alloys Compd. **682**, 381 (2016); Z.-S. Wu, G. Zhou, L.-C. Yin, W. Ren, F. Li, and H.-M. Cheng, Nano Energy **1**(1), 107 (2012); S. Ishaq, M. Moussa, F. Kanwal, M. Ehsan, M. Saleem, T. N. Van, and D. Losic, Sci. Rep. **9**(1), 5974 (2019); Y. Hou, Y. Cheng, T. Hobson, and J. Liu, Nano Lett. **10**(7), 2727 (2010); M. Zhi, C. Xiang, J. Li, M. Li, and N. Wu, Nanoscale **5**(1), 72 (2013).
[17]Z. Du, M. Liu, Y. Li, Y. Chen, and X. Zhong, J. Mater. Chem. A **5**(11), 5577 (2017); A. M. Bazargan, F. Sharif, S. Mazinani, and N. Naderi, J. Mater. Sci.: Mater. Electron. **28**, 2962 (2017); S. Elmas, Ş. Korkmaz, and S. Pat, Appl. Surf. Sci. **276**, 641 (2013).

[18]H. B. Lee, W.-Y. Jin, M. M. Ovhal, N. Kumar, and J.-W. Kang, J. Mater. Chem. C **7**(5), 1087 (2019); Z.-n. Yu, J.-j. Zhao, F. Xia, Z.-j. Lin, D.-p. Zhang, J. Leng, and W. Xue, Appl. Surf. Sci. **257**(11), 4807 (2011); K. Sierros, N. Morris, S. Kukureka, and D. Cairns, Wear **267**, 625 (2009).

[19]C. Luo, Y. Chen, Z. Huang, M. Fu, W. Ou, T. Huang, and K. Yue, Adv. Funct. Mater. **33**, 2304486 (2023); W. Peng, X. Pan, X. Liu, Y. Gao, T. Lu, J. Li, M. Xu, and L. Pan, J. Colloid Interfaces Sci. **634**, 782 (2023).

[20]M. Ghaemi, F. Ataherian, A. Zolfaghari, and S. M. Jafari, Electrochim. Acta **53**(14), 4607 (2008).

[21]A. Sumboja, X. Wang, J. Yan, and P. S. Lee, Electrochim. Acta **65**, 190 (2012).

[22]L. Manjakkal, A. Pullanchiyodan, N. Yogeswaran, E. S. Hosseini, and R. Dahiya, Adv. Mater. **32**(24), 1907254 (2020).

[23]V. Sunil, B. Pal, I. I. Misnon, and R. Jose, Mater. Today: Proc. **46**, 1588 (2021).

[24]J. Liu, J. Wang, C. Xu, H. Jiang, C. Li, L. Zhang, J. Lin, and Z. X. Shen, Adv. Sci. **5**(1), 1700322 (2018).

[25]Z. Xu, L. Kong, Y. Wang, B. Wang, and J. Zhao, Org. Electron. **54**, 94 (2018).

[26]L. Manjakkal, L. Pereira, E. K. Barimah, P. Grey, F. F. Franco, Z. Lin, G. Jose, and R. A. Hogg, Prog. Mater. Sci. **142**, 101244 (2024).

[27]S.-W. Kim and S.-Y. Lee, Energy Environ. Mater. **3**(3), 265 (2020).

21 March 2024 14:35:48